

Seasonal sea ice variability in eastern Fram Strait over the last 2000 years

Patricia Cabedo-Sanz¹ · Simon T. Belt¹

Received: 26 February 2016 / Accepted: 3 June 2016 / Published online: 8 July 2016
© Springer-Verlag Berlin Heidelberg 2016

Abstract We present a high-resolution (ca. 50 years) biomarker-based reconstruction of seasonal sea ice conditions for the West Svalbard continental margin covering the last ca. 2k years. Our reconstruction is based on the distributions of sea ice algal (IP₂₅) and phytoplankton (brassicasterol and HBI III) lipids in marine sediment core MSM5/5-712-1 retrieved in 2007. The individual and combined (PIP₂₅) temporal profiles, together with estimates of spring sea ice concentration [SpSIC (%)] based on a recent calibration, suggest that sea ice conditions during the interval ca. 50–1700 AD may not have been as variable as described in previous reconstructions, with SpSIC generally in the range ca. 35–45 %. A slight enhancement in SpSIC (ca. 50 %) was identified at ca. 1600 AD, contemporaneous with the Little Ice Age, before declining steadily over the subsequent ca. 400 years to near-modern values (ca. 25 %). In contrast to these spring conditions, our data suggest that surface waters during summer months were ice free for the entire record. The decline in SpSIC in recent centuries is consistent with the known retreat of the winter ice margin from documentary sea ice records. This decrease in sea ice is possibly attributed to enhanced inflow of warm water delivered by the North Atlantic Current and/or increasing air temperatures, as shown in previous marine and terrestrial records. Comparison of our biomarker-based sea ice reconstruction with one obtained previously based on dinocyst distributions in a core from a similar location reveals partial agreement in the early–mid part of the records (ca. 50–1700 AD), but a notable divergence in the

most recent ca. 300 years. We hypothesise that this divergence likely reflects the individual signatures of each proxy method, especially as the biomarker-based SpSIC estimates during this interval (<25 %) are much lower than the threshold level (>50 % sea ice cover) used for the dinocyst approach. Alternatively, divergence between outcomes may indicate seasonality shifts in sea ice conditions, such that a combined biomarker-dinocyst approach in future studies might provide further insights into this important parameter.

Keywords IP₂₅ · Sea ice · Biomarker · Proxy · Late Holocene · Fram Strait

Introduction

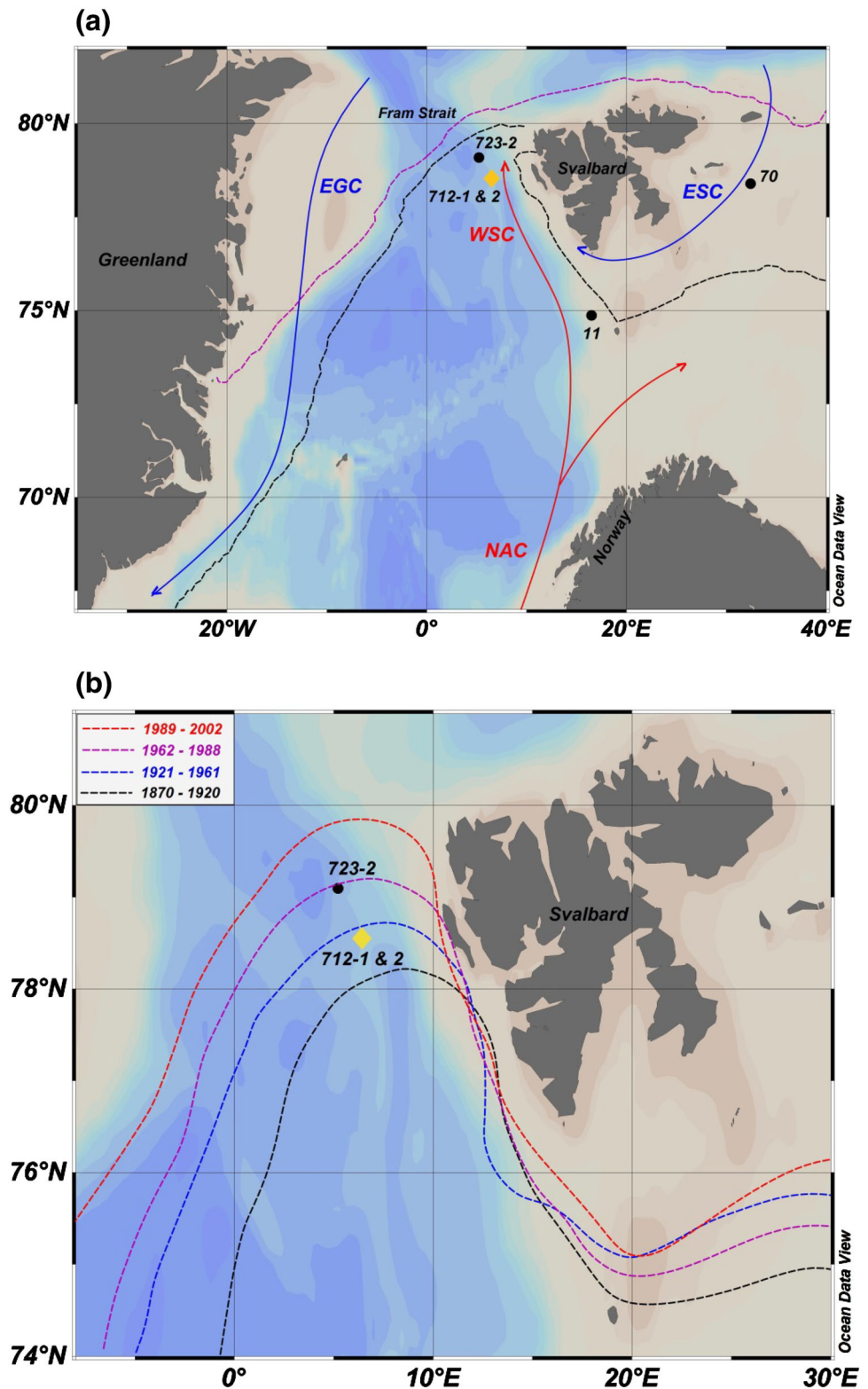
Sea ice and the study region

Sea ice is a critical component of the global climate system, influencing heat, gas and moisture exchange between the oceans and the atmosphere [46], and further contributing to circulation patterns through brine rejection and freshwater release during ice formation and melt, respectively (e.g. [21] and references therein). The observed rapid decline in Arctic sea ice extent and thickness (e.g. [45] has prompted a need to better resolve temporal changes to sea ice in the past, in order that the recent trends can be placed into a better context, and to provide key datasets for improving models of past and future change (e.g. [25, 29]). From a regional perspective, Fram Strait represents a pivotal study location for investigating past changes to sea ice, since it represents the major oceanographic gateway between the Arctic and North Atlantic oceans (Fig. 1a). The two main currents that characterise the region are the

✉ Simon T. Belt
sbelt@plymouth.ac.uk

¹ School of Geography, Earth and Environmental Sciences,
Plymouth University, Drake Circus, Plymouth PL4 8AA, UK

Fig. 1 **a** Map showing the core location under study (yellow diamond): MSM5/5-712-1 (712-1). Other cores mentioned in this paper (black dots) are: MSM5/5-723-2 (723-2, [35]), MSM5/5-712-2 (712-2, [35]), JM09-KA11-GC (11, [6]) and NP05-11-70GC (70, [6]). The core site described in Bonnet et al. [12] is at the same location as core 712-1. The main ocean currents are the cold East Greenland Current (EGC), carried southwards along the east coast of Greenland, and the relatively warm North Atlantic Current (NAC) that flows northward along the northern Norwegian shelf and continues into the Arctic Ocean via the West Spitsbergen Current (WSC). The cold East Spitsbergen Current (ESC) is also indicated. The median sea ice extent (>15 % monthly mean concentration) for March (black line) and September (magenta line) is shown for the period 1981–2010 (National Snow and Ice Data Center, Boulder, Colorado); **b** map showing average April location of the sea ice margins at 1870–1920 AD (black line), 1921–1961 AD (blue line), 1962–1988 AD (magenta line) and 1989–2002 AD (red line) (<http://nsidc.org/data/gis/data.html>; data based on [22])



North Atlantic Current (NAC) and the East Greenland Current (EGC) (Fig. 1a). Northerly flowing warm Atlantic Water is delivered to the Arctic by the NAC via a principal trajectory along the West Svalbard continental margin,

which normally renders eastern Fram Strait relatively free of sea ice, even in winter. In contrast, western Fram Strait is characterised by cold, ice-laden waters as a result of sea ice export from the Arctic Ocean via the EGC. Arctic

Water also flows along the east coast of Svalbard to the south and west of Spitsbergen, delivering sea ice via the East Spitsbergen Current (ESC) [26, 31]. The magnitude of heat delivery by the NAC plays a critical role in determining the precise sea ice conditions in eastern Fram Strait. For example, increased Atlantic Water inflow during the last ca. 120 years [42] has been associated with a general trend of reduced sea ice cover in the Arctic and, more locally, a northerly retreat of the winter ice margin (Fig. 1b, [22]). A further impact of the NAC on sea ice conditions in the region, more generally, is that seasonal shifts in the position of the winter and summer ice margins are significantly less pronounced than for the central and eastern Barents Sea, which are dominated by low temperature and salinity Arctic Water [26]. The latter regions also experience seasonal ice cover from autumn to spring, before retreating, rapidly, during late spring/summer. As such, the region as a whole experiences contrasting seasonal sea ice cover [47], which is influenced, in part, by the strength of the NAC [26].

Motivated, in part, by the sensitivity of oceanographic and atmospheric conditions in Fram Strait towards climatic change, a number of proxy-based studies have been carried out in recent years that have provided new insights into the centennial- and millennial-scale paleoceanographic evolution along the West Svalbard continental margin (e.g. [12]; 28; [33, 35, 42, 48]). These investigations have benefited from the recovery of high accumulation rate (and well-dated) marine sediments, which have enabled the application of an array of biological and mineralogical proxies for the determination of atmospheric and oceanic temperatures, salinity, and sea ice cover [12, 33, 35, 38, 42, 49].

Our objective in the current study is to add to the existing suite of previous paleoceanographic investigations for West Svalbard, by presenting a high-resolution (ca. 50 years) biomarker-based reconstruction of sea ice conditions spanning the last ca. 2k years. In particular, we build on recent developments in biomarker-based approaches to sea ice reconstruction by providing both descriptive and semi-quantitative estimates of spring sea ice concentration [SpSIC (%)]. Biomarker-based sea ice reconstructions for the West Svalbard margin have been performed previously through analysis of sediments from the same or similar locations, although these focused mainly on longer timeframes (e.g. Holocene and post-LGM; [33, 35]) and did not provide information for recent centuries. In addition, semi-quantitative estimates of SpSIC were only tentative [35]. A dinocyst-based record of mean annual sea ice duration (months/year) for the last 2k years for West Svalbard has previously been presented by Bonnet et al. [12], however, and we make comparisons between this and our biomarker-based record as part of the current study.

Background to biomarker proxy method

In recent years, the organic geochemical marker IP₂₅ (Ice Proxy with 25 carbon atoms; [7]) has emerged as a particularly suitable proxy method for carrying out Arctic sea ice reconstructions, and in the determination of past seasonal sea ice cover, in particular (e.g. [8–10, 16, 43]). IP₂₅ is a mono-unsaturated highly branched isoprenoid (HBI) lipid produced by certain Arctic sea ice diatoms [15], and is found commonly in Arctic and sub-Arctic marine sediments underlying seasonal sea ice cover [34, 36, 44, 50, 51]. Identification of IP₂₅ in the geological record (Arctic marine sediments), therefore, provides a convincing case for the past occurrence of seasonal sea ice, while variability in IP₂₅ content is generally associated with corresponding fluctuations in seasonal sea ice extent (e.g. [8]). The absence of IP₂₅ in Arctic and sub-Arctic settings is less straightforward to interpret, although either of permanent ice cover or ice-free conditions have been suggested as potential settings (e.g. [8, 43, 50]). In any case, the co-measurement of certain phytoplankton biomarkers (including sterols such as brassicasterol) can provide additional information about low-ice or open-water conditions. In addition, combining IP₂₅ and phytoplankton marker concentrations in the form of the so-called PIP₂₅ index [34] has the potential to provide even more detailed or semi-quantitative estimates of sea ice conditions than from the individual biomarkers alone. The use of brassicasterol as a phytoplankton biomarker when calculating PIP₂₅ indices is not without problems, however, since it may also be derived from non-marine sources, and its (generally) much higher sedimentary abundance necessitates the use of a balance factor in the PIP₂₅ calculation (see Sect. “Biomarker analyses”), which can cause problems of consistency, in particular (see [6, 8] for further details). Since these limitations may not be relevant in all cases, the adoption of a further phytoplankton marker, possessing a more selective source and which has sedimentary concentrations closer to those of IP₂₅, might represent a suitable complementary approach, at least. Indeed, Belt et al. [6] recently demonstrated that a further tri-unsaturated HBI lipid (C_{25:3} or HBI III) derived from certain diatoms may be a more suitable phytoplankton marker for use within the PIP₂₅ index, following analysis of lipid distributions in surface sediments from the Barents Sea experiencing variable seasonal sea ice cover. Smik et al. [41] subsequently showed that PIP₂₅ indices based on IP₂₅ and HBI III (i.e. P_{III}IP₂₅) exhibit a strong linear correlation to SpSIC in the Barents Sea, thus providing a potential means of reconstructing semi-quantitative SpSIC (%) estimates for this region, at least. In the current study, we therefore measured concentrations of IP₂₅, brassicasterol and HBI III in a ¹⁴C-dated sediment core (MSM5/5-712-1) retrieved from the West Svalbard margin in 2007 and used P_{III}IP₂₅

indices together with the recent calibration of Smik et al. [41] to obtain estimates of SpSIC (%) for the last 2k years.

Materials and methods

Field methods and chronology

Core MSM5/5-712-1 was recovered from the West Svalbard continental margin (78°54.94N, 6°46.04E, water depth 1490.5 m, core length 46 cm; Fig. 1a) during cruise leg MSM5/5 on board the R/V Maria S. Merian in the summer of 2007. The age model is based on five ^{14}C accelerator mass spectrometry (AMS) radiocarbon dates presented and described previously [42].

Biomarker analyses

In total, 43 downcore sediment samples were analysed for the biomarkers IP₂₅, HBI III and brassicasterol. Sampling and analyses were carried out at 1 cm intervals representing the last ca. 2k years, with a resolution of ca. 50 years. Biomarker analyses (HBI and sterol lipids) were performed using methods described previously [4, 6]. Briefly, two internal standards were added to each freeze-dried sediment sample to permit quantification of lipid biomarkers. 9-octylheptadec-8-ene (9-OHD, 10 μL ; 10 $\mu\text{g mL}^{-1}$) was added for quantification of HBI lipids (IP₂₅ and HBI III), while 5 α -androstan-3 β -ol (10 μL ; 10 $\mu\text{g mL}^{-1}$) was added for quantification of brassicasterol. Samples were then extracted using dichloromethane/methanol (3 \times 3 mL; 2:1 v/v) and ultrasonication. Following removal of the solvent from the combined extracts using nitrogen, the resulting total organic extracts (TOE) were purified using column chromatography (silica), with HBIs (hexane; 6 mL) and brassicasterol (20:80 methylacetate/hexane; 6 mL) collected as two fractions. Analysis of individual fractions was carried out using gas chromatography–mass spectrometry (GC–MS) and operating conditions were as described previously (e.g. [4, 13]). Brassicasterol was derivatized (BSTFA; 50 μL ; 70 °C; 1 h) prior to analysis by GC–MS. Mass spectrometric analyses were carried out either in total ion current (TIC) or single ion monitoring (SIM) mode. The identification of IP₂₅ [7] and HBI III [3] was based on their characteristic GC retention indices and mass spectra. Quantification of lipids was achieved by comparison of mass spectral responses of selected ions (SIM mode, IP₂₅, m/z 350; HBI III, m/z 346; brassicasterol, m/z 470) with those of the internal standards (9-OHD, m/z 350; 5 α -androstan-3 β -ol, m/z 333) and normalised according to their respective response factors and sediment masses [4]. Analytical reproducibility was monitored using a standard sediment with known abundances of biomarkers for every

20 sediment samples extracted (analytical error 6 %, $n = 2$). PIP₂₅ values were calculated using Eq. 1 according to the method of Müller et al. [34]. Similarly, the c factor used in the PIP₂₅ calculation was obtained from the ratio of the mean concentrations of IP₂₅ and each phytoplankton biomarker (i.e. brassicasterol and HBI III; Eq. 2). Estimates of SpSIC (%) were calculated using the P_{III}IP₂₅ data and the recent calibration of Smik et al. [41] (Eq. 3). Although the study site is located somewhat beyond the main boundary of the region investigated by Smik et al. [41], we believe that our estimates of SpSIC (and the temporal changes to these) based on this calibration are, nonetheless, realistic, including reasonably good agreement between values from the core-top and known SpSIC obtained from satellite records (see “Discussion” for further details). A summary of all data can be found in Table 1.

$$\text{PIP}_{25} = \text{IP}_{25} / (\text{IP}_{25} + cP). \quad (1)$$

$$c = \text{mean IP}_{25} / \text{mean P}. \quad (2)$$

$$\text{SpSIC (\%)} = (\text{P}_{\text{III}}\text{IP}_{25} - 0.0692) / 0.0107. \quad (3)$$

Results

IP₂₅, HBI III and brassicasterol were present in all sedimentary horizons throughout the record although some variability in concentrations was observed for all three biomarkers. Thus, concentrations of IP₂₅, HBI III and brassicasterol were in the ranges 1.6–3.4, 2.2–4.7 and 340–590 ng g⁻¹, respectively (Fig. 2a–c) and all three biomarkers showed a general in-phase fluctuation from ca. 50 to 1750 AD. An increase in IP₂₅, HBI III and brassicasterol concentrations was observed from ca. 5 to 400 AD, followed by a decline in all three biomarkers from ca. 400 to 700 AD and an interval of relatively low biomarker concentrations between ca. 700 and 800 AD (Fig. 2a–c). After ca. 800 AD, all biomarkers increased in concentration until ca. 1350 AD, before declining again up to ca. 1750 AD. However, a small lag in the decline of IP₂₅ values was observed when compared to those of HBI III and brassicasterol (Fig. 2a–c). In contrast, IP₂₅ concentrations remained generally low after ca. 1750 AD, whereas HBI III and brassicasterol concentrations increased towards the present. In addition, P_{III}IP₂₅ values and estimates of SpSIC (%) values remained reasonably consistent (ca. 0.45–0.57 and 35–45 %, respectively) (Fig. 2d, e) between ca. 50 and 1400 AD. After ca. 1400 AD, P_{III}IP₂₅ and SpSIC values increased to ca. 0.6 and 50 %, respectively, especially between ca. 1500 and 1600 AD, before steadily decreasing towards modern times (Fig. 2d, e), where they both reached their lowest values in the entire record.

Table 1 Summary of depth-age relationship for core MSM5/5-712-1 [42], individual biomarker concentrations, PIP indices and SpSIC estimates based on Smik et al. [41]

Depth (cm)	Age (year AD)	IP ₂₅ (ng/g sed)	HBI III (ng/g sed)	Brassicasterol (ng/g sed)	P _{III} IP ₂₅	P _B IP ₂₅	SpSIC (% estimate)
0.5	1989	1.74	4.52	537.89	0.35	0.37	26.23
1.5	1953	1.85	4.24	517.12	0.38	0.40	28.98
2.5	1917	1.88	3.59	476.89	0.42	0.42	33.06
3.5	1881	2.18	4.35	525.58	0.41	0.43	31.98
4.5	1844	2.33	3.78	533.97	0.46	0.45	36.81
5.5	1808	1.64	2.74	490.21	0.46	0.38	36.07
6.5	1772	1.77	2.70	423.61	0.48	0.43	38.22
7.5	1736	1.70	2.61	356.85	0.48	0.47	38.05
8.5	1700	1.94	2.60	426.20	0.51	0.46	41.23
9.5	1664	1.81	2.33	381.19	0.52	0.47	42.21
10.5	1628	2.44	2.78	586.62	0.55	0.43	45.06
11.5	1591	2.66	2.56	383.87	0.59	0.56	48.83
12.5	1555	2.58	2.47	403.81	0.59	0.54	49.00
13.5	1519	2.98	3.32	403.42	0.56	0.58	45.53
14.5	1483	3.36	3.71	401.48	0.56	0.61	45.74
15.5	1434	2.87	4.31	440.30	0.48	0.55	38.62
16.5	1380	3.00	4.50	498.79	0.48	0.53	38.59
17.5	1327	3.11	4.09	528.96	0.52	0.52	41.68
18.5	1273	3.21	4.10	566.54	0.52	0.51	42.34
19.5	1220	2.84	4.23	494.85	0.48	0.51	38.75
20.5	1166	2.67	4.10	409.91	0.48	0.54	38.06
21.5	1112	2.77	4.26	368.18	0.48	0.58	38.06
22.5	1062	2.17	3.38	379.31	0.47	0.51	37.69
23.5	1012	2.52	3.19	472.13	0.52	0.50	42.58
24.5	961	2.01	2.36	365.75	0.54	0.50	44.31
25.5	911	2.31	2.66	456.81	0.55	0.48	44.79
26.5	861	2.76	3.23	462.86	0.54	0.52	44.35
27.5	811	1.78	2.51	358.61	0.50	0.48	40.10
28.5	760	2.27	2.31	343.19	0.58	0.55	47.60
29.5	710	2.28	3.10	342.05	0.51	0.55	40.89
30.5	660	2.22	3.03	379.04	0.51	0.52	40.85
31.5	609	2.50	3.39	424.15	0.51	0.52	40.96
32.5	558	2.48	3.92	521.59	0.47	0.47	37.36
33.5	507	2.84	3.53	475.42	0.53	0.52	42.93
34.5	455	2.63	3.20	378.37	0.53	0.56	43.48
35.5	404	2.98	3.80	405.45	0.52	0.57	42.39
36.5	353	2.74	4.69	435.58	0.45	0.54	35.55
37.5	302	2.26	3.78	469.60	0.45	0.47	36.04
38.5	251	2.32	3.03	385.57	0.52	0.53	41.82
39.5	200	2.02	2.48	419.61	0.53	0.47	43.31
40.5	149	1.77	2.18	379.34	0.53	0.46	43.20
41.5	98	1.75	2.26	341.86	0.52	0.48	42.01
42.5	47	1.75	2.16	343.51	0.53	0.48	43.19

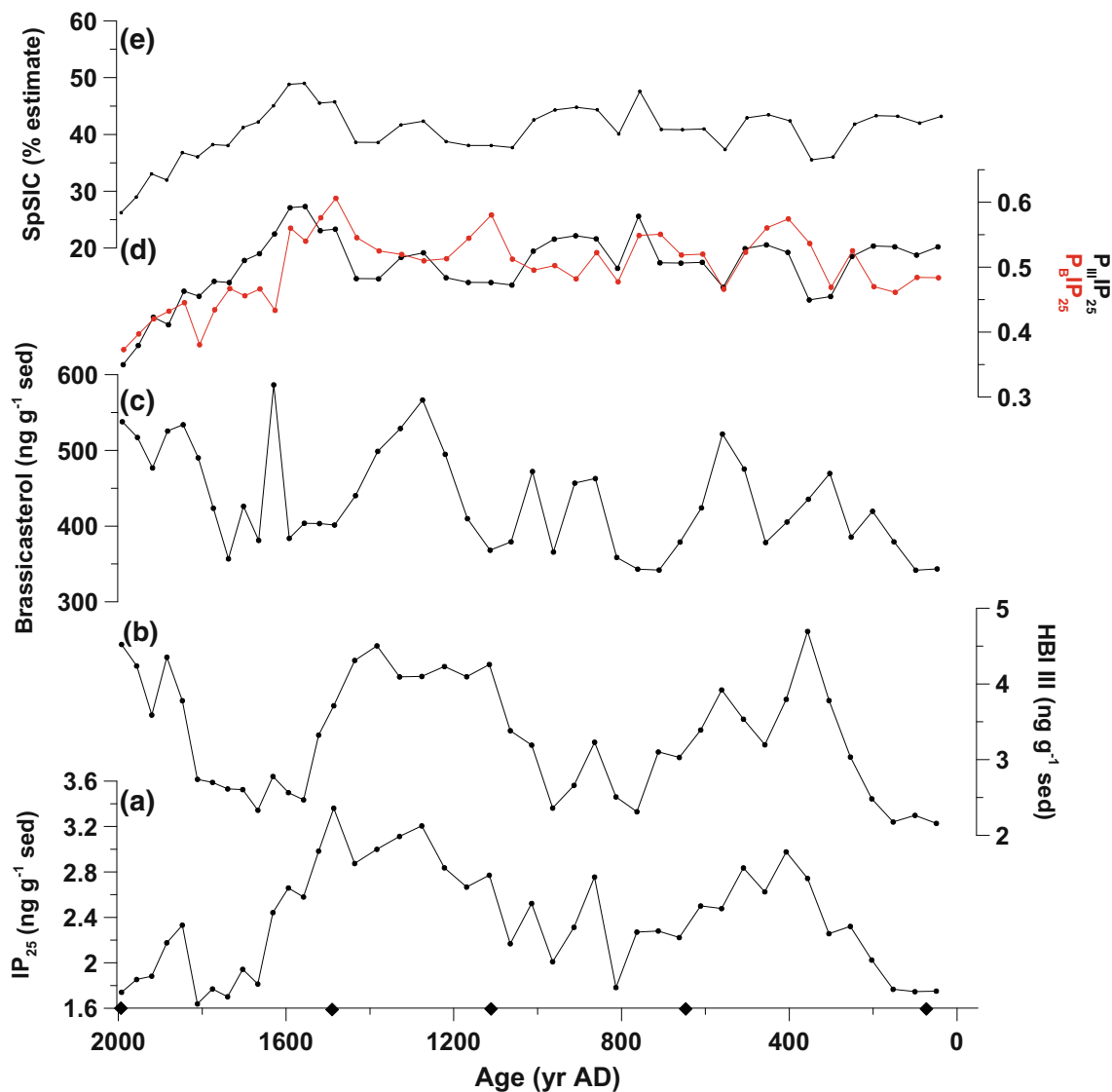


Fig. 2 Temporal concentration profiles of **a** IP₂₅; **b** HBI III; **c** brassicasterol; **d** PIP₂₅ indices calculated using phytoplankton markers HBI III (P_{III}IP₂₅) and brassicasterol (P_BIP₂₅); **e** SpSIC (%) based on Smik et al. [41]

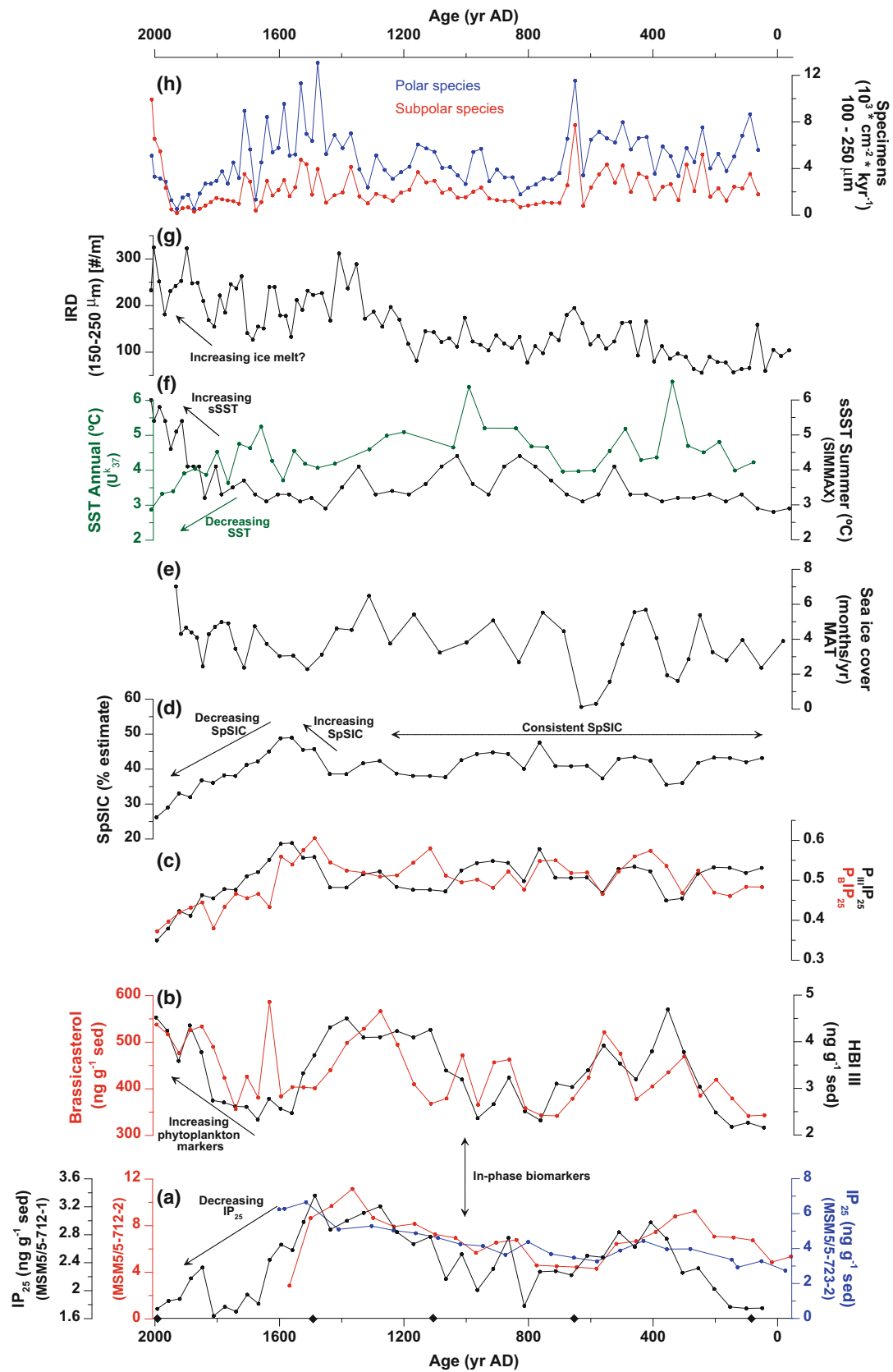
Discussion

Principal outcomes in terms of sea ice conditions

The occurrence of the sea ice biomarker IP₂₅ in all sedimentary horizons analysed provides strong evidence that the MSM5/5-712-1 core site experienced seasonal sea ice cover as a consistent hydrographic feature over the last ca. 2k years. P_BIP₂₅ and P_{III}IP₂₅ profiles were generally in-phase, indicating that both brassicasterol and HBI III are probably suitable as phytoplankton marker counterparts to IP₂₅ for eastern Fram Strait in recent millennia. However, although IP₂₅ concentrations and PIP₂₅ indices suggest somewhat variable sea ice conditions, the range in our estimates of SpSIC (ca. 25–50 %) (Fig. 3d) implies that

Fig. 3 Compilation of proxy data from MSM5/5-712-1 and related cores from the study region. Data are for MSM5/5-712-1 unless otherwise stated. **a** IP₂₅ concentrations in MSM5/5-712-1 (black line), MSM5/5-712-2 (red line, [35]) and MSM5/5-723-2 (blue line, [35]); **b** HBI III and brassicasterol concentrations; **c** PIP₂₅ indices calculated using phytoplankton markers HBI III (P_{III}IP₂₅) and brassicasterol (P_BIP₂₅); **d** SpSIC (%) based on Smik et al. [41]; **e** dinocyst-based sea ice cover (months/year) derived from a further core at the same location as MSM5/5-712-1 [12]; **f** SST and sSST (°C) derived from alkenones [38] and planktic foraminifera [42], respectively; **g** IRD in the 150–250 µm fraction [49]; **h** fluxes of polar and subpolar planktic foraminifers (100–250 µm fraction) [42, 49]

such variability in sea ice for the West Svalbard margin in recent millennia may have been less extreme than predicted from other proxy records (e.g. [49]), and certainly less than the broad range of sea ice extent for the site throughout the



Holocene deduced from a previous study [35]. For the majority of the early–mid part of the record (ca. 50–1400 AD), estimates of SpSIC are reasonably constant (ca. 35–45 %), before an increase to ca. 50 % during the period ca. 1500–1600 AD, contemporaneous with the Little Ice Age (Fig. 3d). Following this increase, SpSIC shows a steady reverse trend after ca. 1660 AD, which extends to the modern era. Interestingly, this declining trend reflects the general reduction in sea ice and a northward retreat of the maximum winter sea ice extent described in documentary records over the last ca. 150 years [22], while our SpSIC estimates for the top of the core (ca. 25 %) are only slightly higher than the mean SpSIC derived from satellite records for this region of Fram Strait over the last ca. 30 years (10–15 %; NSIDC). Since this interval also corresponds to the upper few centimetres of the core, this slight overestimate in SpSIC might be a consequence of bioturbation in the upper sections, with partial incorporation of older material with higher IP_{25} . Given that $P_{III}IP_{25}$ indices are all well below the lower limit threshold (0.8) suggested recently to be indicative of summer sea ice occurrence [41], we also conclude that summer surface waters remained ice free during the entire record. Further, our data suggest that, since ca. 1900 AD, SpSIC along the West Svalbard margin has diminished to its lowest values in the last 2k years, consistent with a coeval and markedly enhanced inflow of warm Atlantic Water to the Arctic Ocean [42] and rising air temperatures derived from marine [38] and terrestrial (e.g. [18]) records.

Comparisons with other proxy data

The availability of an array of other proxy data for the MSM5/5-712-1 core and related locations enables us to place our new sea ice reconstruction into further context and provide an updated picture of the oceanographic conditions for the West Svalbard margin over the last 2k years. Although some consistency between different proxy datasets and alignment with well-known climate epochs (e.g. the Little Ice Age) exists, this is not always the case (e.g. [2, 27, 49]). As such, we categorise the temporal paleo-oceanographic evolution for the last 2k years into two main intervals, with reference to certain named epochs, where useful.

Early–mid part of the record (ca. 50–1750 AD)

In the earliest part of the record (ca. 50–700 AD), the increase in IP_{25} , brassicasterol and HBI III concentrations towards ca. 400 AD (Fig. 3a, b) suggests a transition from unfavourable conditions for all three biomarkers to one that has a positive influence over the production of both sea ice algae and phytoplankton (viz. ice edge or marginal ice zone

(MIZ) conditions). On the basis of enhanced (but variable) planktic foraminiferal fluxes (Fig. 3h), Werner et al. [49] suggested that this transitional phase represented a general amelioration of conditions from heavy sea ice cover (ca. 120 BC–1 AD) to one with a fluctuating summer ice margin, and our individual biomarker data appear consistent with this interpretation. Further, surface and sub-surface temperatures [38, 42] increase during this phase (Fig. 3f), which are also indicative of a general reduction in sea ice. In contrast, a decline in all three biomarkers from ca. 400 to 700 AD is accompanied by a slight cooling trend in the alkenone-derived SST record (Fig. 3f), possibly reflecting a return to increased overall sea ice cover. Indeed, between ca. 700 and 800 AD, generally reduced biomarker content coincides with relatively low foraminifera fluxes (Fig. 3h), yet high proportions of polar species (i.e. *N. pachyderma*; [49]). Previously, the latter was interpreted as indicating extended sea ice cover, despite there also being evidence for sub-surface advection of Atlantic Water during the same interval [49].

After ca. 800 AD, the increase in all three biomarkers until ca. 1350 AD (Fig. 3a, b) suggests a further return to less severe, MIZ conditions, an interpretation supported by a generally warmer surface layer (Fig. 3f) and increases to sub-polar planktic foraminifera (Fig. 3h) [49]. However, Werner et al. [49] interpreted the distributions and isotopic composition of planktic foraminifera, together with relatively low IRD from ca. 900 to 1350 AD, as indicative of ice-free conditions, yet our biomarker data suggest seasonal ice cover, even if some estimates of SpSIC from ca. 1100 to 1400 AD are slightly lower (ca. 35 %) than the immediately preceding and subsequent intervals (Fig. 3d). In fact, despite the aforementioned reversible transitions between (apparently) extended sea ice cover and MIZ conditions between ca. 50 and 1300 AD, our estimates of SpSIC remain remarkably consistent (ca. 40 %; Fig. 3d) throughout this interval, indicating that factors other than SpSIC are likely to have had influences over biomarker distributions. Although such factors are currently unidentified, it is interesting, for example, that the alternating trend in biomarker concentrations seen between ca. 50 and 1350 AD is broadly reflected by the alkenone-derived SST record (Fig. 3f), while the seasonal sea ice dynamics may also exert significant control (see later).

The decline in all three biomarkers after ca. 1350 AD indicates a possible further return to enhanced sea ice cover and likely marks the transition into the LIA seen in numerous other North Atlantic marine records (e.g. [2, 11, 23]; 39). However, the decline in IP_{25} exhibits a slight lag compared to the phytoplankton markers (Fig. 3a, b) suggesting that the transition in sea ice conditions may have been somewhat different to those described previously. This lag in decreasing IP_{25} concentration is also

apparent in the PIP_{25} data, with maximum values around 1600 AD, reflecting a positive deviation in SpSIC to ca. 50 %, before declining to more typical values (ca. 40 %) after a further ca. 100 years (Fig. 3d). In addition, this relatively brief interval of enhanced SpSIC is accompanied by lower SST (alkenone) and sSST (planktic foraminifera) (Fig. 3f). After ca. 1600 AD, a decline in the concentration of all three biomarkers possibly suggests a return to enhanced sea ice cover, despite a reduction in the SpSIC and a slight increase in both SST and sSST (Fig. 3f).

A clear feature of the temporal fluctuations in individual biomarker concentrations from ca. 0 to 1750 AD is their in-phase temporal coherence (Fig. 3a, b), demonstrating that changes to sea ice conditions impacted somewhat equally (directionally) for both IP_{25} and phytoplankton markers. In some previous IP_{25} -based sea ice reconstructions, e.g. [6, 16, 24, 32], often opposing trends in IP_{25} and phytoplankton biomarker profiles have been observed, and interpreted in terms of transitions between intervals of increased sea ice cover (high IP_{25} , low phytoplankton marker) and reduced ice extent (low IP_{25} , high phytoplankton marker). However, consistent with the current data from the West Svalbard margin, Müller et al. [35] previously reported in-phase changes in IP_{25} and phytoplankton marker concentrations in a Holocene record from the same site and interpreted such a scenario as indicative of a rapidly fluctuating ice margin. Further, Collins et al. [17] arrived at a similar conclusion for glacial sea ice conditions in the Southern Ocean, adding that in-phase biomarker trends may also be indicative of low sea ice seasonality. For the current study, such an interpretation may, therefore, represent a preferred alternative to one of the more extreme exchanges between extended sea ice cover versus MIZ conditions, as described earlier here, and previously [49], especially since IP_{25} and the phytoplankton markers are all present throughout the record. In addition, our estimates of SpSIC (ca. 35–45 %) (Fig. 3d) and previous determinations of sea ice duration (ca. 2–6 months/year) (Fig. 3e) based on dinocysts in a core from the same site [12] both indicate seasonal, rather than extended, ice cover. In-phase trends within individual biomarker profiles generally have the impact of reducing variability in PIP_{25} (and SpSIC) that may, potentially, lead to an underestimation of the changes in sea ice conditions implied from IP_{25} alone. However, for the MSM5/5-712-1 core, changes in IP_{25} concentration are also relatively small, especially when compared to those seen in longer Holocene records from the same and nearby sites (MSM5/5-712-2 and MSM5/5-723-2; [35]), both of which exhibit similar IP_{25} profiles to our data for the overlapping period (Fig. 3a). Thus, IP_{25} concentration changes by an order of magnitude from the early to late Holocene in the MSM5/5-712-2 record [35],

while values covering the last ca. 2k years in all three cores only vary by a factor of two, at most (Fig. 3a). Of course, a fluctuating ice margin has much closer parallels with the modern sea ice cycle for the region, with a significantly smaller change in the position of the winter and summer ice margins than, for example, the neighbouring Barents Sea (Fig. 1a). Interestingly, peak total foraminifera fluxes (Fig. 3h), previously interpreted as representing ice edge settings by comparison with modern datasets [49], also broadly coincide with increased biomarker concentrations, consistent with a strong biological coupling between the surface and sub-surface environments.

The last 250 years (since ca. 1750 AD)

According to our biomarker data, conditions after ca. 1750 AD did not parallel the early–mid part of the record, with generally low IP_{25} concentrations accompanied by increasing phytoplankton marker abundances, especially after ca. 1800 AD. Such changes are particularly apparent through declining PIP_{25} values and SpSIC, but it is also evident that surface (alkenone) and sub-surface (planktic foraminifera) temperatures diverge during this latter part of the LIA, with a clear cooling trend observed for the former (Fig. 3f). The occurrence of generally opposing trends between IP_{25} and HBI III (and brassicasterol) since ca. 1750 AD contrasts the earlier part of the record and previous longer-term Holocene sea ice records from the region [35]. However, this divergence in IP_{25} and phytoplankton biomarkers is reminiscent of the distributions of IP_{25} and HBI III in surface sediments and downcore records (e.g. core sites 11 and 70; Fig. 1a) from the Barents Sea, with low IP_{25} and high HBI III, in particular, associated with ice edge retreat within the MIZ during spring [6]. We suggest, therefore, that from ca. 1750 AD to modern, surface conditions at the West Svalbard margin transcended from higher seasonal sea ice cover (i.e. ca. 40 % SpSIC), to a winter ice edge scenario with reduced SpSIC (ca. 25 % or less).

Our observation of declining SpSIC since ca. 1600 AD is also consistent with the suggestion by Rueda et al. [38] that reduced surface temperatures and increasing air and sub-surface temperatures, especially in the last ca. 500 years, may have coincided with a trend of increasing sea ice melt and, thus, SpSIC. Increased air temperatures have also been reconstructed for neighbouring (terrestrial) West Spitsbergen, with concomitant glacial advance attributed to enhanced precipitation [18] that we suggest may also have been associated with reduced sea ice cover. Alternatively, lower SSTs in the recent record may reflect an earlier seasonal bloom due to lower sea ice conditions as suggested previously to explain apparent anomalies in

SSTs for the North Icelandic Shelf and coastal settings around Newfoundland in the Labrador Sea [39, 40]. In any case, the apparently increased de-coupling between the surface and sub-surface temperature records since ca. 1750 AD likely reflects a period of most significant change in sea ice conditions, with cooler and fresher surface waters resulting from melting sea ice, possibly as a result of warmer air temperatures as suggested by Rueda et al. [38]. It is also noted that IRD content reached its highest values after ca. 1750 AD (Fig. 3g), a further indicator of increasing sea ice melt, although an additional contribution to the IRD budget from icebergs derived from Svalbard glaciers cannot be discounted, e.g. [1, 49].

Biomarker versus dinocyst approaches to sea ice reconstruction

As a final discussion point, we compare our biomarker-based sea ice reconstruction with one based on dinocysts in a further core obtained from the same site (Fig. 3e; [12]). Inspection of the temporal profile for dinocyst-based sea ice duration (Fig. 3e) with those of biomarkers (individual or PIP₂₅; Fig. 3a–c) or SpSIC (Fig. 3d) reveals no clear or consistent agreement, even factoring in potential age-control offsets between the two cores. Although some parallels might exist in the early–mid parts of the dinocyst and SpSIC records (ca. 50–1400 AD; Fig. 3d, e), this is not the case for the later profiles, and after ca. 1600 AD, in particular, with reconstructions exhibiting generally opposing trends. In the most recent parts of the records, for example, our estimates of lowest SpSIC align with the northerly retreat of the winter sea ice margin over the last ca. 150 years (Fig. 1b; [22]), yet apparently contradict an enhancement in sea ice duration in the dinocyst record (Fig. 3e). Further, the reconstruction of Bonnet et al. [12] implies ice-free conditions ca. 550–700 AD, while our data suggest SpSIC of ca. 40 % for the same interval. Inconsistencies in proxy records are not uncommon, however, and a number of discrepancies have already been reported and discussed for surface temperature and salinity reconstructions based on foraminifera and dinocysts in different cores from the study location [12, 49]. Such differences are not necessarily straightforward to resolve, but may potentially arise from influences associated with seasonally dependent proxy responses, changes to water column sub-structure, variable depth habitat of native flora and fauna, or appropriateness of transfer functions, which may exhibit a strong regional dependence. Inconsistencies between biomarker- and dinocyst-based sea ice reconstructions have been reported previously and loosely attributed to the possible different signatures that each proxy represents (e.g. [8, 19, 30, 37]). Outcomes from the current study might

help further direct this debate. For example, the dinocyst-based method yields semi-quantitative estimates of sea ice duration in months of sea ice (with >50 % cover)/year [20], while the corresponding reconstructions based on IP₂₅ are intrinsically associated with spring sea ice conditions [5, 14] and, more quantitatively, seasonal (spring) sea ice concentration, as described here and previously [6, 34, 36, 41, 50]. For the current study, we also note that SpSIC is almost exclusively below the threshold level for dinocyst-based methods (>50 % sea ice cover) in any case, so differences between outcomes are not entirely unexpected. It is also feasible that while there might be some scenarios for which sea ice duration and SpSIC are reasonably in-phase, divergence in their respective proxy records may reflect an effective de-coupling between them, especially during intervals of amplified seasonality. For example, for the West Svalbard margin, we speculate that increasing sea ice duration, yet declining SpSIC, seen in the last ca. 300 years, may have arisen due to larger seasonal shifts between generally colder winters and warmer summer temperatures that would have particularly impacted on spring ice melt. Consistent with this suggestion, increasing air temperatures from marine [38] and terrestrial [18] records for the region since ca. 1600 AD coincide with the reduction in SpSIC shown here. The combination of new biomarker-based approaches for estimating SpSIC with complementary methods of determining sea ice duration may, therefore, offer additional insights into seasonal shifts in sea ice occurrence that are not necessarily available from either individual proxy. Such approaches would clearly benefit from further dinocyst and biomarker investigations on the same sediments.

Conclusions

Our biomarker-based reconstruction of sea ice conditions for the West Svalbard continental margin covering the last ca. 2k years suggests that changes to sea ice conditions during this interval may not have been as extreme as reported in previous proxy-based studies, especially for the interval ca. 50–1700 AD, with SpSIC generally ca. 40 % throughout. An increase in SpSIC to ca. 50 % was observed at ca. 1600 AD, however, which we attribute to slightly enhanced sea ice cover during the LIA. SpSIC returned to more typical values at ca. 1750 AD, before declining further towards modern values (ca. 25 %), consistent with observational records of a northerly retreat of the winter sea ice limit in the last ca. 150 years [22]. The general in-phase behaviour of the sea ice algal and phytoplankton markers observed for the majority of the record (ca. 50–1750 AD) is indicative of a fluctuating ice margin

and relatively low sea ice seasonality. In contrast, a divergence in trends of the same biomarkers since ca. 1750 AD is interpreted in terms of an amplified seasonal sea ice cycle and a rapid ice edge retreat within the MIZ during the spring, thus providing a model for the sea ice conditions for the West Svalbard margin in recent centuries. Such a contrast in the relative temporal trends of sea ice and pelagic biomarkers has been observed in related sea ice reconstructions (e.g. [6, 32]) and may prove to be an additionally useful tool when deducing or refining paleo sea ice conditions. Improvements to such paleo sea ice descriptions, and temporal changes to these, will also help in the further refinement of other proxy-based inferences of surface environments, in particular, and may potentially help clarify (or resolve) reconstructions of broader water column features for sea ice covered settings.

Acknowledgments We thank the University of Plymouth for financial support and Dr. Robert Spielhagen for sampling the MSM5/5-712-1 core. We are also grateful to two anonymous reviewers who provided a number of useful comments that helped improve the quality of the manuscript. This work is a contribution to the CASE Initial Training Network funded by the European Community's 7th Framework Programme FP7 2007/2013, Marie-Curie Actions, under Grant Agreement No. 238111.

References

- Andersen ES, Dokken TM, Elverhøi A, Solheim A, Fossen I (1996) Late Quaternary sedimentation and glacial history of the western Svalbard continental margin. *Mar Geol* 133:123–156
- Andersson C, Risebrobakken B, Jansen E, Dahl SO (2003) Late Holocene surface ocean conditions of the Norwegian Sea (Vøring Plateau). *Paleoceanography* 18:1044
- Belt ST, Allard WG, Massé G, Robert JM, Rowland SJ (2000) Highly branched isoprenoids (HBIs): identification of the most common and abundant sedimentary isomers. *Geochim Cosmochim Acta* 64:3839–3851
- Belt ST, Brown TA, Navarro Rodriguez A, Cabedo Sanz P, Tonkin A, Ingle R (2012) A reproducible method for the extraction, identification and quantification of the Arctic sea ice proxy IP₂₅ from marine sediments. *Anal Method* 4:705–713
- Belt ST, Brown TA, Ringrose AE, Cabedo-Sanz P, Mundy CJ, Gosselin M, Poulin M (2013) Quantitative measurement of the sea ice diatom biomarker IP₂₅ and sterols in Arctic sea ice and underlying sediments: further considerations for palaeo sea ice reconstruction. *Organ Geochem* 62:33–45
- Belt ST, Cabedo-Sanz P, Smik L, Navarro-Rodriguez A, Berben SM, Knies J, Husum K (2015) Identification of paleo Arctic winter sea ice limits and the marginal ice zone: optimised biomarker-based reconstructions of late Quaternary Arctic sea ice. *Earth Planet Sci Lett* 431:127–139
- Belt ST, Massé G, Rowland SJ, Poulin M, Michel C, LeBlanc B (2007) A novel chemical fossil of palaeo sea ice: IP₂₅. *Organ Geochem* 38:16–27
- Belt ST, Müller J (2013) The Arctic sea ice biomarker IP₂₅: a review of current understanding, recommendations for future research and applications in palaeo sea ice reconstructions. *Quat Sci Rev* 79:9–25
- Belt ST et al (2010) Striking similarities in temporal changes to spring sea ice occurrence across the central Canadian Arctic Archipelago over the last 7000 years. *Quat Sci Rev* 29:3489–3504
- Berben SMP, Husum K, Cabedo-Sanz P, Belt ST (2014) Holocene sub centennial evolution of Atlantic water inflow and sea ice distribution in the western Barents Sea. *Clim Past* 10:181–198
- Berstad IM, Sejrup HP, Klitgaard-Kristensen D, Hafflidason H (2003) Variability in temperature and geometry of the Norwegian Current over the past 600 years; stable isotope and grain size evidence from the Norwegian margin. *J Quat Sci* 18:591–602
- Bonnet S, de Vernal A, Hillaire-Marcel C, Radi T, Husum K (2010) Variability of sea-surface temperature and sea-ice cover in the Fram Strait over the last two millennia. *Mar Micropaleontol* 74:59–74
- Brown TA, Belt ST (2012) Identification of the sea ice diatom biomarker IP₂₅ in Arctic benthic macrofauna: direct evidence for a sea ice diatom diet in Arctic heterotrophs. *Polar Biol* 35:131–137
- Brown TA, Belt ST, Philippe B, Mundy CJ, Massé G, Poulin M, Gosselin M (2011) Temporal and vertical variations of lipid biomarkers during a bottom ice diatom bloom in the Canadian Beaufort Sea: further evidence for the use of the IP₂₅ biomarker as a proxy for spring Arctic sea ice. *Polar Biol* 34:1857–1868
- Brown TA, Belt ST, Tatarek A, Mundy CJ (2014) Source identification of the Arctic sea ice proxy IP₂₅. *Nat Commun* 5:4197. doi:10.1038/ncomms5197
- Cabedo-Sanz P, Belt ST, Knies J, Husum K (2013) Identification of contrasting seasonal sea ice conditions during the Younger Dryas. *Quat Sci Rev* 79:74–86
- Collins LG, Allen CS, Pike J, Hodgson DA, Weckström K, Massé G (2013) Evaluating highly branched isoprenoid (HBI) biomarkers as a novel Antarctic sea-ice proxy in deep ocean glacial age sediments. *Quat Sci Rev* 79:87–98
- D'Andrea WJ, Vaillancourt DA, Balascio NL, Werner A, Roof SR, Retelle M, Bradley RS (2012) Mild Little Ice Age and unprecedented recent warmth in an 1800 years lake sediment record from Svalbard. *Geology* 40:1007–1010
- de Vernal A, Gersonde R, Goosse H, Seidenkrantz M-S, Wolff EW (2013) Sea ice in the paleoclimate system: the challenge of reconstructing sea ice from proxies—an introduction. *Quat Sci Rev* 79:1–8
- de Vernal A, Rochon A, Fréchette B, Henry M, Radi T, Solignac S (2013) Reconstructing past sea ice cover of the Northern Hemisphere from dinocyst assemblages: status of the approach. *Quat Sci Rev* 79:122–134
- Dickson R, Rudels B, Dye S, Karcher M, Meincke J, Yashayaev I (2007) Current estimates of freshwater flux through Arctic and subarctic seas. *Prog Oceanogr* 73:210–230
- Divine DV, Dick C (2006) Historical variability of sea ice edge position in the Nordic Seas. *J Geophys Res* 111:C01001
- Eiriksson J et al (2006) Variability of the North Atlantic current during the last 2000 years based on shelf bottom water and sea surface temperatures along an open ocean/shallow marine transect in western Europe. *Holocene* 16:1017–1029
- Fahl K, Stein R (2012) Modern seasonal variability and deglacial/Holocene change of central Arctic Ocean sea-ice cover: new insights from biomarker proxy records. *Earth Planet Sci Lett* 351–352:123–133
- Goosse H, Roche DM, Mairesse A, Berger M (2013) Modelling past sea ice changes. *Quat Sci Rev* 79:191–206
- Hopkins TS (1991) The GIN sea—a synthesis of its physical oceanography and literature review 1972–1985. *Earth Sci Rev* 30:175–318
- Isaksson E et al (2005) Two ice-core $\delta^{18}\text{O}$ records from Svalbard illustrating climate and sea-ice variability over the last 400 years. *Holocene* 15:501–509

28. Jernas P, Klitgaard Kristensen D, Husum K, Wilson L, Koç N (2013) Palaeoenvironmental changes of the last two millennia on the western and northern Svalbard shelf. *Boreas* 42:236–255
29. Johannessen OM et al (2004) Arctic climate change: observed and modelled temperature and sea ice variability. *Tellus A* 56:328–341
30. Ledu D, Rochon A, de Vernal A, St-Onge G (2010) Holocene paleoceanography of the northwest passage, Canadian Arctic Archipelago. *Quat Sci Rev* 29:3468–3488
31. Loeng H (1991) Features of the physical oceanographic conditions of the Barents Sea. *Polar Res* 10:5–18
32. Müller J, Massé G, Stein R, Belt ST (2009) Variability of sea-ice conditions in the Fram Strait over the past 30,000 years. *Nat Geosci* 2:772–776
33. Müller J, Stein R (2014) High-resolution record of late glacial and deglacial sea ice changes in Fram Strait corroborates ice-ocean interactions during abrupt climate shifts. *Earth Planet Sci Lett* 403:446–455
34. Müller J, Wagner A, Fahl K, Stein R, Prange M, Lohmann G (2011) Towards quantitative sea ice reconstructions in the northern North Atlantic: a combined biomarker and numerical modelling approach. *Earth Planet Sci Lett* 306:137–148
35. Müller J, Werner K, Stein R, Fahl K, Moros M, Jansen E (2012) Holocene cooling culminates in sea ice oscillations in Fram Strait. *Quat Sci Rev* 47:1–14
36. Navarro-Rodriguez A, Belt ST, Knies J, Brown TA (2013) Mapping recent sea ice conditions in the Barents Sea using the proxy biomarker IP₂₅: implications for palaeo sea ice reconstructions. *Quat Sci Rev* 79:26–39
37. Polyak L, Belt ST, Cabedo-Sanz P, Yamamoto M, Park Y-H (2016) Holocene sea-ice conditions and circulation at the Chuckchi–Alaskan margin, Arctic Ocean, inferred from biomarker proxies. *Holocene*. doi:[10.1177/0959683616645939](https://doi.org/10.1177/0959683616645939)
38. Rueda G, Fietz S, Rosell-Melé A (2013) Coupling of air and sea surface temperatures in the eastern Fram Strait during the last 2000 years. *Holocene* 23(5):692–698
39. Sicre MA et al (2011) Sea surface temperature variability in the subpolar Atlantic over the last two millennia. *Paleoceanography* 26:PA4218
40. Sicre MA et al (2014) Labrador current variability over the last 2000 years. *Earth Planet Sci Lett* 400:26–32
41. Smik L, Cabedo-Sanz P, Belt ST (2016) Semi-quantitative estimates of paleo Arctic sea ice concentration based on source-specific highly branched isoprenoid alkenes: a further development of the PIP₂₅ index. *Organ Geochem* 92:63–69
42. Spielhagen RF et al (2011) Enhanced modern heat transfer to the Arctic by warm Atlantic water. *Science* 331:450–453
43. Stein R, Fahl K, Müller J (2012) Proxy reconstruction of cenozoic Arctic ocean sea-ice history—from IRD to IP₂₅. *Polarforschung* 82:37–71
44. Stoyanova V, Shanahan TM, Hughen KA, de Vernal A (2013) Insights into circum-Arctic sea ice variability from molecular geochemistry. *Quat Sci Rev* 79:63–73
45. Stroeve JC, Serreze MC, Holland MM, Kay JE, Malanik J, Barrett AP (2012) The Arctic's rapidly shrinking sea ice cover: a research synthesis. *Clim Chang* 110:1005–1027
46. Thomas DN, Dieckmann GS (2010) *Sea ice*, 2nd edn. Wiley Blackwell Publishing, New York
47. Vinje T (1977) Sea ice conditions in the European sector of the marginal seas of the Arctic, 1966–1975. *Norsk Polarinst, Arbok* 1975:163–174
48. Werner K, Spielhagen RF, Bauch D, Hass HC, Kandiano E (2013) Atlantic water advection versus sea-ice advances in the eastern Fram Strait during the last 9 ka: multiproxy evidence for a two-phase Holocene. *Paleoceanography* 28:283–295
49. Werner K, Spielhagen RF, Bauch D, Hass HC, Kandiano E, Zamelczyk K (2011) Atlantic water advection to the eastern Fram Strait—multiproxy evidence for late Holocene variability. *Palaeogeogr Palaeoclimatol Palaeoecol* 308:264–276
50. Xiao X, Fahl K, Müller J, Stein R (2015) Sea-ice distribution in the modern Arctic ocean: biomarker records from trans-Arctic ocean surface sediments. *Geochim Cosmochim Acta* 155:16–29
51. Xiao X, Fahl K, Stein R (2013) Biomarker distributions in surface sediments from the Kara and Laptev seas (Arctic Ocean): indicators for organic-carbon sources and sea-ice coverage. *Quat Sci Rev* 79:40–52